Structural, Surface, and Optical Properties of $Sm_xBi_{2-x}Fe_4O_9$

Sanjay Ramteke[1] and Amol Nande[2]*

[1] S. P. College, Chandrapur, India

[2] G. N. College of Science, Ballarpur, India

Abstract:

In this work, $Sm_xBi_{2-x}Fe_4O_9$(x=0.02, 0.04, 0.06, 0.08, and 0.10) compound synthesized using microwave assisted sol-gel method. The samples were characterized using X-ray diffractionSpectrometer, Fourier-Transform Infra-Red Spectroscopy and Ultra Violet- Visible spectroscopy. The structural confirmed the crystals structure and purity of the sample using X-ray diffractionSpectrometer. The analysis confirmed the formation of orthorhombic structure with (211) is the most favorable orientation. Surface analysis confirmed the presence of nitrate group and –OH group along with all expected Bismuth and Ferrous oxides. The analysis confirmed the presence of Bi-O, Bi-O-Bi, Fe-O, and FeO_4tetrahedra. The Ultra Violet- Visible spectral analysis showed that the band-gap values can be estimated. Also, the estimated refractive index in ultra-violet region was 2.04.

Keywords: Band-gap, FTIR, $Bi_2Fe_4O_9$

Introduction

Rare-earth doped inorganic semiconductors have potential application in photocatalysis, optical and magnetic fields as well as in field of solar cells and photovoltaic cells. As the most of the famous inorganic materials have poor sunlight harvesting leading to the lower efficiencies. This was due to comparative wide bandgap. This led to the scope for the researchers to explore new inorganic materials which have band gap sensitive to visible light to enhance the efficiencies.

Bismuth based complex oxides such as $BiFeO_3$ and $Bi_2Fe_4O_9$ shows comparatively small band gaps which facilitate them to work in visible and UV light range [1-3]. Especially, $Bi_2Fe_4O_9$ provide feasibility in easy synthesis process which has known orthorhombic structure with Pbam space group. The structure formed from FeO_6octahedra interconnected to Fe_2O_7 double tetrahedral units and BiO_6 group in alternating order along c-axis [4, 5]. The materials can be synthesized using many simple techniques such as hydrothermal, solid state reaction, Pechini, solvothermal and pulsed laser deposition method[6-11].

It was observed that the doping of rare-earth metal ion in $Bi_2Fe_4O_9$increase its electrical and optical properties, as the doping reduces the oxygen vacancy contents. Ibrahim et al. [4]

showed that Sm doped $Bi_2Fe_4O_9$nanoplates had semiconductor features. The conduction mechanism was governed by electrons and small polaron hopping at low and high temperature. Also, reduction in charge defects was observed. Rao et al. [12]Nd doped $Bi_2Fe_4O_9$ compound in which narrow band gap was observed leading to enhance electrical and optical properties. Rao et al. [13] synthesized Gd doped $Bi_2Fe_4O_9$ compound using ball milling method. The research work depicted with doping conduction improved which confirmed by observed narrow band gap. Also, in other work, Rao et al. [14] showed that in the compound had enhancement in conducting electron-hole hopping which responsible for enhancement in photocatalytic degradation efficiency.

In this work, Sm-doped $Bi_2Fe_4O_9$ were synthesized using microwave assisted sol-gel method. The synthesized samples were taken for X-ray diffraction spectroscopy (XRD), Fourier-Transform Infra-Red spectroscopy (FTIR) and Ultra Violet- Visible spectroscopy (UV-Vis). These characterization were useful for studying structural, surface and optical properties.

Experimental

The series of $Sm_xBi_{2-x}Fe_4O_9$compound with (x=0.02, 0.04, 0.06, 0.08, and 0.10) were synthesized using microwave assisted sol-gel method.The starting materials were Samarium Nitrate ($Sm(NO_3)_3$), Bismuth Nitrate ($Bi(NO_3)_3{\cdot}5H_2O$), Ferric nitrate ($Fe(NO_3)_3(H_2O)_9$), and Urea. All mentioned starting materials were in high purity phase.Firstly, the stoichiometric amounts of all mentioned metal nitrates and urea were dissolved in deionized water. The obtained mixture were stirred using magnetic stirrer for 10 min at 30 °C giving brownish homogeneous solution. Later, the solution heated using microwave for 3 hrs until the solution burnt and turned to foamy brown ash. Once the obtained ash cooled down to room temperature, it crushed for 4 hrs using mortar and pastel to obtain crystalline brown powder. The crystalline powder annealed at 800 °C for 8 hrs in muffle furnace. At last, the sample cooled down to room temperature and again crushed for 4 hrs. The samples stored in tubes to avoid from moisture. The prepared sample series underwent various characterization techniques including X-ray diffraction, UV-Visible spectroscopy, and Fourier transform infrared spectroscopy.

Result and Discussion

Structural Analysis

The structural analysis of Sm-doped $Bi_2Fe_4O_9$compound is performed using XRD patterns as shown in figure 1. The observed XRD data are well matched with the standard pdf card number 1530918. This confirmed that the crystal structure of the prepared samples is orthorhombic in nature with space group Pbam (55). The expected lattice parameters are a=7.94 Å, b = 8.44 Å, and c= 6.01Å and the expected volume of the unit cell is 402.752 $Å^3$. It can be said that the addition of Sm to $Bi_{2-x}Fe_4O_9$ unit cell does not make huge difference in the structural properties as the addition of dopant with different concentration does not change the

patter and peak positions of XRD patterns. Also, the $Bi_{2-x}Fe_4O_9$ unit cell is formed due to evenly distribution of FeO_6^-octahedral shape and FeO_4^-tetrahedral shape groups. Moreover, eight oxygen atoms surrounds the Bi^+ metal ions to form short BiO_3 and long BiO_5 orthogonal unit cells [6, 15, 16].

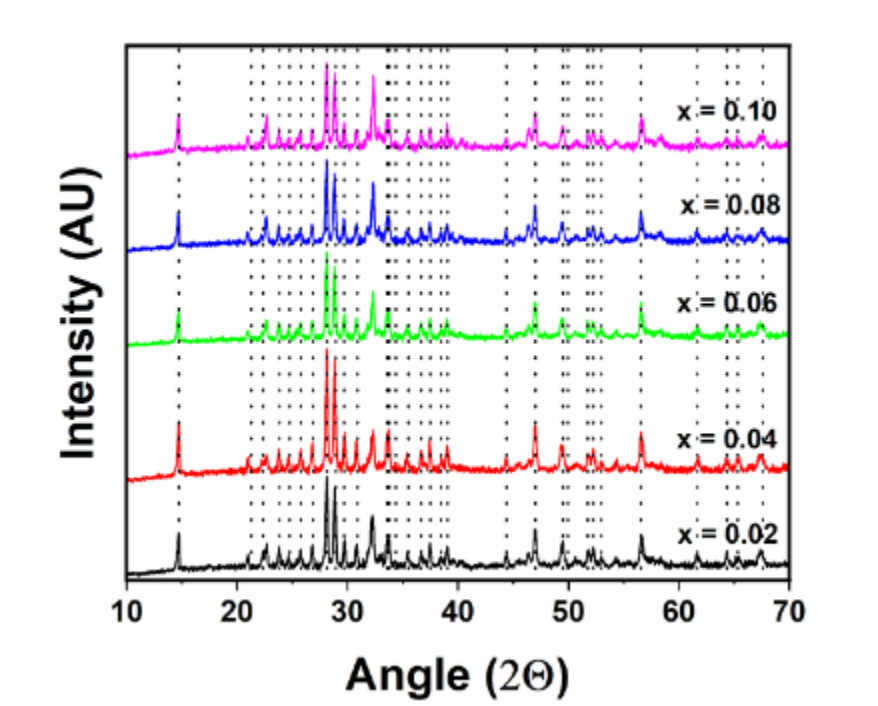

Figure 1 XRD data for $Sm_xBi_{2-x}Fe_4O_9$ (x=0.02, 0.04, 0.06, 0.08, and 0.10) compound.

All observed diffraction peaks with corresponding peaks are listed in Table 1. Out of which all diffraction planes, (211) planes centered at 28.15° diffraction points is the most intense peak for all Sm concentrations of the $Bi_{2-x}Fe_4O_9$compound referring the most favorable orientation direction during crystallization of the sample.

Table 1. The observed diffraction peaks with corresponding diffraction planes observed for al synthesized samples are listed here.

SN	Diffraction Peak	Planes	SN	Diffraction Peak	Planes
1	14.73	(001)	17	37.51	(202)
2	21.3	(111)	18	38.45	(122)
3	22.38	(200)	19	39.05	(212)
4	23.86	(120)	20	44.39	(140)
5	24.76	(210)	21	47.02	(141)
6	25.78	(021)	22	49.51	(411)
7	26.89	(201)	23	49.96	(232)
8	28.15	(121)	24	51.77	(123)
9	28.93	(211)	25	52.24	(213)
10	29.71	(002)	26	52.98	(042)
11	30.9	(220)	27	56.58	(412)
12	33.58	(112)	28	61.68	(004)
13	33.77	(130)	29	64.37	(342)
14	34.39	(221)	30	65.33	(432)
15	35.52	(310)	31	67.58	(512)
16	36.68	(022)			

FTIR Analysis

The FTIR analysis provides valuable information about chemical structures and functional groups present on surface of the samples. Figure 2 depicts the FTIR spectra for $Sm_xBi_{2-x}Fe_4O_9$ (x=0.02, 0.04, 0.06, 0.08, and 0.10) compounds in a frequency range of 4000 – 400 cm^{-1}.The figures depicts multiple absorption peaks between 3500 – 1500 cm^{-1} attributing to stretching vibration of –OH group from water molecules mostly available from synthesis process[17]. However, absorption bands near 1517 cm^{-1} were mainly due to the presence of nitrate group residual from the synthesis process[18]. The absorption peaks present between 1200 – 600 cm^{-1} regions suggested to be fingerprint region in which each compound has their unique vibrations. For our samples we observed peaks at 815, 713, and 542 cm^{-1} absorption peaks which were due to vibration, bending and stretching of Bi-O and Fe-O presents in different forms. The absorption peak present near 800 cm^{-1} could be due to C-O stretching as well as due to stretching vibration of Fe-O bonds present in the FeO_4tetrahedra[17, 19].The absorption peak at 713 cm^{-1} is due to Bi-O-Bi and Bi-O bending mode [20]. Also, the absorption peak closer to the 542 cm^{-1} frequency was due to the O-Fe-O bending vibration of the FeO_4tetrahedra[21]. All

observed peaks were consistent for all molar Sm concentrations. Furthermore, all observed absorption peaks were well with the mentioned in the literature.

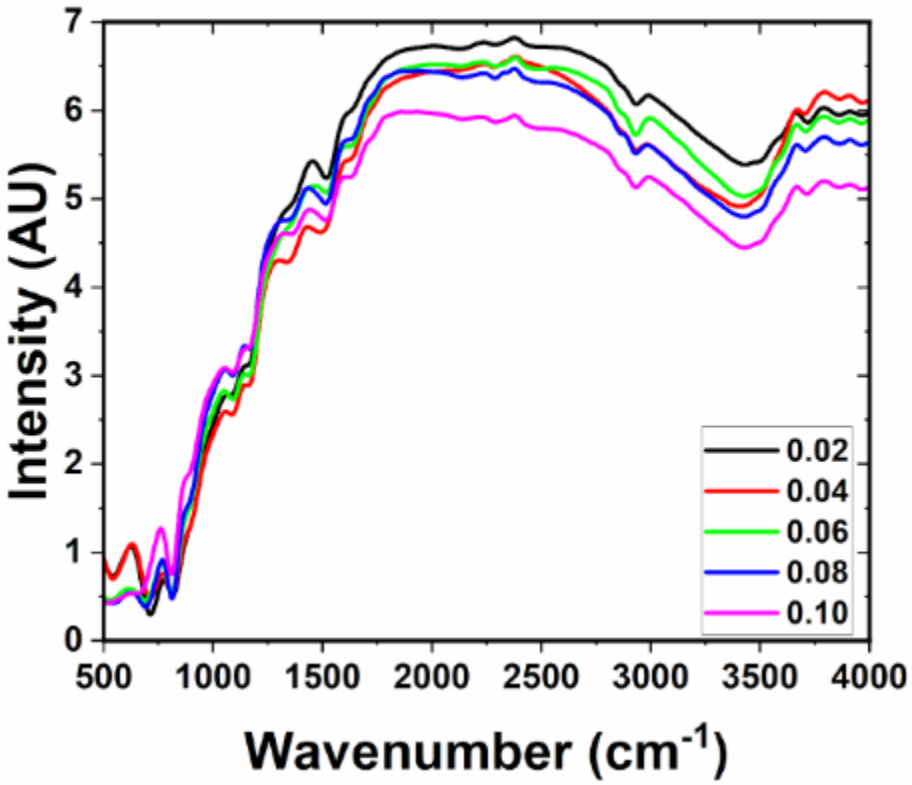

Figure 2FTIR spectra for $Sm_xBi_{2-x}Fe_4O_9$ (x=0.02, 0.04, 0.06, 0.08, and 0.10) compound.

UV-Visible analysis

The optical absorption property of inorganic compounds are very important to deal with many other properties such as photocatalysis and others as these are associated with the optical band-gap. Figure 3 shows UV-visible spectra for $Sm_xBi_{2-x}Fe_4O_9$ (x=0.02, 0.04, 0.06, 0.08, and 0.10) compounds measured between 200 – 1000 nm wavelength range. Two distinguished absorption peaks are visible for all Sm concentrations of the samples referring to the tetrahedral and octahedral crystal fields of 3d orbitals of the Fe crystals [3].

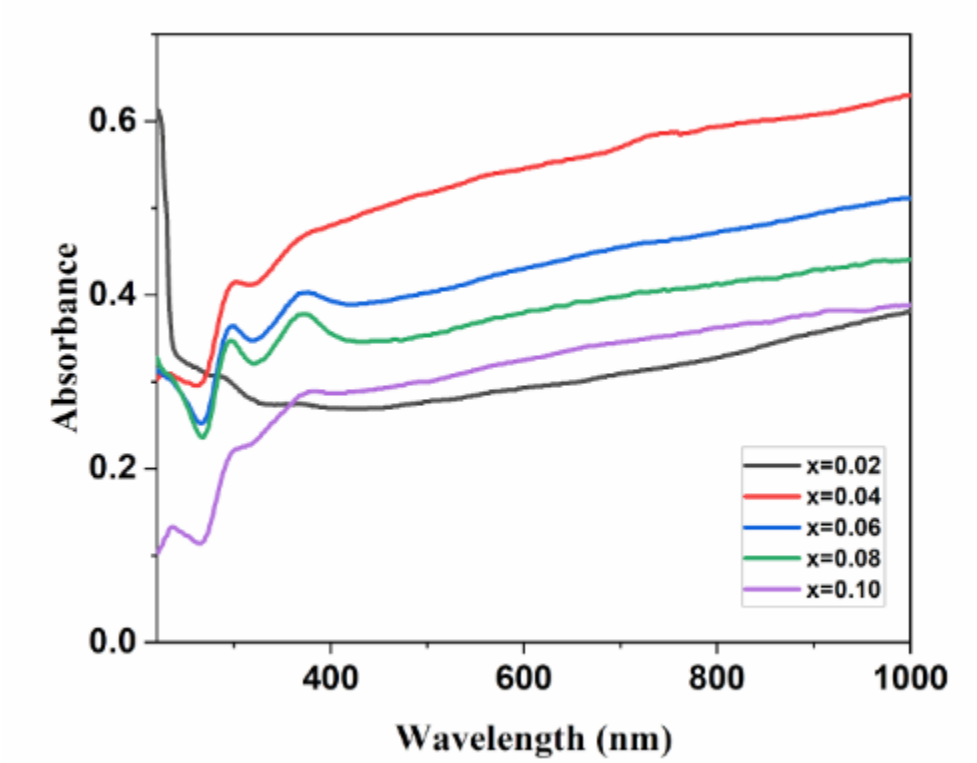

Figure 3 UV-visible sectra for $Sm_xBi_{2-x}Fe_4O_9$ (x=0.02, 0.04, 0.06, 0.08, and 0.10) compound.

The band gap can be estimated using Tau's plot which plotted considering equation $\alpha hv = B(hv - Eg)^{n/2}$. Here, α, h, v, B, and Eg are the coefficient of absorption, Plank's constant, frequency of light, semiconductor constant and semiconductor band-gap respectively. The transition parameter n can have 1 values for allowed transition band gap[22, 23]. The respective plot is plotted between $(\alpha hv)^2$ verses hv an example of the plot for $Sm_xBi_{2-x}Fe_4O_9$ (x = 0.08) is shown in Figure 4.Three band gaps were observed for the phosphor 2.45, 3.23, and 4.24 eV. For all series of samples the energy gaps are varied as 2.35 – 2.51 eV, 3.19 – 3.35 eV, and 4.10 – 4.26 eV.

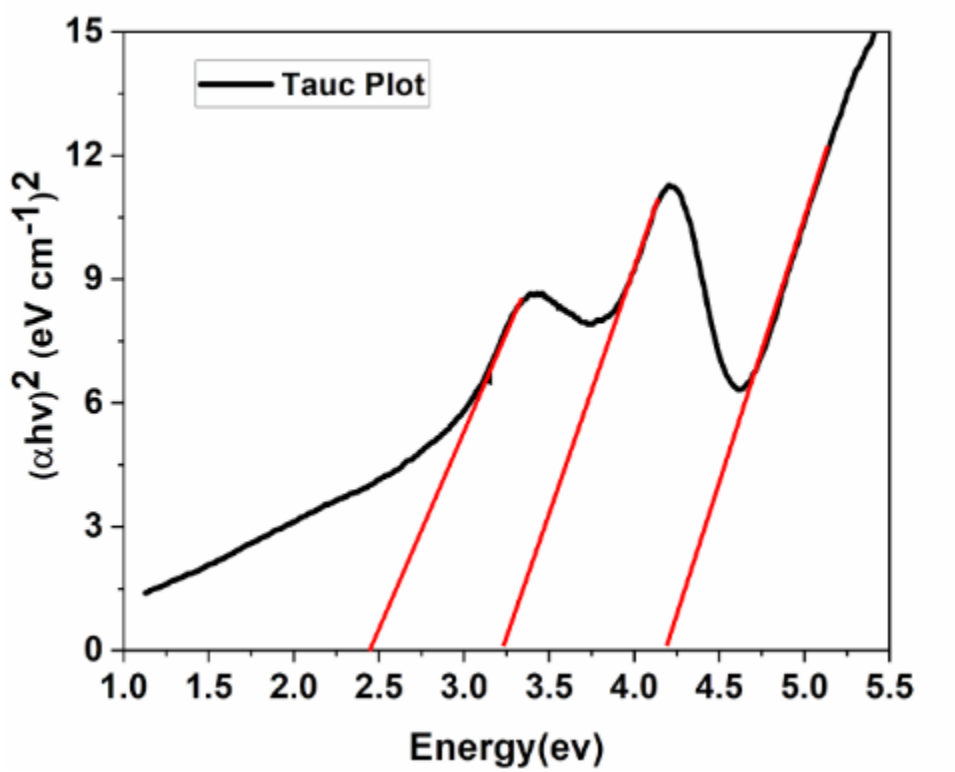

Figure 4 Tau plot for $Sm_xBi_{2-x}Fe_4O_9$ (x= 0.08) compounds

It is possible to estimate refractive index using Herve and vandamme relation $R.I. = \sqrt{\left[1 + \left(\frac{X}{Eg+Y}\right)\right]}$[24, 25]. Here, X and Y are constant and their values respectively are 13.6 and 3.4 eV. The estimated refractive index in UV region is 2.04.

Conclusion

The above analysis confirmed the Sm doped $Bi_2Fe_4O_9$ compound were successfully synthesized using microwave assisted sol-gel method. XRD analysis confirmed the formation of Sm doped $Bi_2Fe_4O_9$ compound with orthorhombic crystal structure. The unit cell of the compound was formed due to the FeO_6 octahedral shapes, and FeO_4 tetrahedral shapes as well as Bi atoms were surrounded by eight oxygen atoms. Out of all observed plane. (211) is most dominating orientation for all Sm dopant concentration. FTIR analysis confirmed the presence of Fe-O, FeO4, Bi-O-Bi, and Bi-O groups in which absorption peaks were observed for vibration, bending and stretching of these groups. The data is consistent with the literature. In UV-Visible spectra, two distinguished absorption peaks were observed which were due to the 3d-orbital of Fe crystal depicting the tetrahedral and octahedral crystal field. The estimated three band gap vales were estimated for each UV-Visible graph which felt in range of 2.35 – 2.51 eV, 3.19 – 3.35 eV, and 4.10 – 4.26 eV. These energy gap are suitable in ultraviolet and visible region

suggesting the prepared samples have photocatalytic and photovoltaic application in these regions. The refractive index also estimated as 2.04.

References

[1] A. Alemi and A. Purhasan, "Synthesis and characterization of single phase Bi1−xSmx/2Dyx/2FeO3 (x = 0 and 0.015) and Bi2−xSmx/2Dyx/2Fe4O9 (x = 0 and 0.03) powders via sol–gel method,"*Journal of Materials Science: Materials in Electronics,* vol. 28, no. 19, pp. 14476-14482, 2017/10/01 2017, doi: 10.1007/s10854-017-7310-y.

[2] X. Wang, M. Zhang, P. Tian, W. Chin, and C. Zhang, "A facile approach to pure-phase Bi2Fe4O9 nanoparticles sensitive to visible light,"*Applied surface science,* vol. 321, pp. 144-149, 2014.

[3] X. Wang, M. Zhang, P. Tian, W. S. Chin, and C. M. Zhang, "A facile approach to pure-phase Bi2Fe4O9 nanoparticles sensitive to visible light,"*Applied Surface Science,* vol. 321, pp. 144-149, 2014/12/01/ 2014, doi: https://doi.org/10.1016/j.apsusc.2014.09.166.

[4] E. Ibrahim, G. Farghal, M. M. Khalaf, and H. M. A. El-Lateef, "Enhanced Magnetic and DC Electrical Properties of Sm-Doped Bi2Fe4O9 Nanoplates Synthesized by Sol–Gel Method,"*Nano,* vol. 15, no. 02, p. 2050020, 2020.

[5] K. L. Da Silva, V. Šepelák, A. Paesano Jr, F. J. Litterst, and K. D. Becker, "Structural studies of Bi2 (FexAl1–x) 4O9 solid solutions (0.1≤ x≤ 1.0) prepared by a combined mechanochemical/thermal synthesis," ed: Wiley Online Library, 2010.

[6] E. M. M. Ibrahim, G. Farghal, M. M. Khalaf, and H. M. A. El-Lateef, "Enhanced Magnetic and DC Electrical Properties of Sm-Doped Bi2Fe4O9 Nanoplates Synthesized by Sol–Gel Method,"*Nano,* vol. 15, no. 02, p. 2050020, 2020, doi: 10.1142/s1793292020500204.

[7] T. Wang *et al.*, "The synthesis and microstructural, optical, magnetic characterizations of m 0 0-oriented epitaxial Bi2Fe4O9 thin film by pulsed laser deposition,"*Materials Letters,* vol. 204, pp. 81-84, 2017.

[8] S. Lavasani, O. Mirzaee, H. Shokrollahi, A. Moghadam, and M. Salami, "Magnetic and morphological characterization of Bi2Fe4O9 nanoparticles synthesized via a new reverse chemical co-precipitation method,"*Compounds International,* vol. 43, no. 15, pp. 12120-12125, 2017.

[9] T. Wu, L. Liu, M. Pi, D. Zhang, and S. Chen, "Enhanced magnetic and photocatalytic properties of Bi2Fe4O9 semiconductor with large exposed (001) surface,"*Applied Surface Science,* vol. 377, pp. 253-261, 2016.

[10] S. Huang, Y. Qiu, and S. Yuan, "Enhanced magnetization and electric polarization in Bi2Fe4O9 compounds by magnetic field pre-sintering,"*Materials Letters,* vol. 160, pp. 323-326, 2015.

[11] S. Huang *et al.*, "Effect of Al3+ substitution on the structural, magnetic, and electric properties in multiferroic Bi2Fe4O9 compounds,"*Journal of Solid State Chemistry*, vol. 227, pp. 79-86, 2015.

[12] S. Krishna Rao *et al.*, "Investigation of room temperature multi-functional properties of Nd doped mullite Bi2Fe4O9,"*Vacuum*, vol. 172, p. 109109, 2020/02/01/ 2020, doi: https://doi.org/10.1016/j.vacuum.2019.109109.

[13] S. K. Rao *et al.*, "Unraveling the potential of Gd doping on mullite Bi2Fe4O9 for fiber optic ethanol gas detection at room temperature,"*Materials Chemistry and Physics*, vol. 278, p. 125646, 2022/02/15/ 2022, doi: https://doi.org/10.1016/j.matchemphys.2021.125646.

[14] K. Subha Rao *et al.*, "Delineating the photocatalytic properties of doped mullite Bi2Fe4O9 by virtue of Gd3+ ions,"*Materials Letters*, vol. 297, p. 129960, 2021/08/15/ 2021, doi: https://doi.org/10.1016/j.matlet.2021.129960.

[15] H. Zhang, X. Chen, T. Wang, F. Wang, and W. Shi, "Structure and electrical properties of BiFeO3 thin films grown on LaNiO3 electrode by chemical solution deposition,"*Journal of alloys and compounds*, vol. 500, no. 1, pp. 46-48, 2010.

[16] H. Dai *et al.*, "Studies on the structural, electrical and magnetic properties of Ce-doped BiFeO3 compounds,"*Journal of Alloys and Compounds*, vol. 672, pp. 182-189, 2016.

[17] M. Kong, H. Song, F. Li, D. Dai, and H. Gao, "Facile synthesis of Bi2Fe4O9 nanoplate and its application as a novel adsorbent for Cu(II) removal,"*Journal of Environmental Chemical Engineering*, vol. 5, no. 1, pp. 69-78, 2017/02/01/ 2017, doi: https://doi.org/10.1016/j.jece.2016.11.020.

[18] E. A. Bruns *et al.*, "Comparison of FTIR and particle mass spectrometry for the measurement of particulate organic nitrates,"*Environmental science & technology*, vol. 44, no. 3, pp. 1056-1061, 2010.

[19] D. Cai, J. Li, T. Tong, D. Jin, S. Yu, and J. Cheng, "Phase evolution of bismuth ferrites in the process of hydrothermal reaction,"*Materials Chemistry and Physics*, vol. 134, no. 1, pp. 139-144, 2012.

[20] M. Selvapandiyan and K. Sathiyaraj, "Synthesis, Preparation, Structural, Optical, Morphological and Elemental Analysis of Bismuth Oxides Nanoparticles,"*Silicon*, vol. 12, no. 10, pp. 2309-2315, 2020/10/01 2020, doi: 10.1007/s12633-019-00327-x.

[21] Z.-T. Hu, J. Liu, X. Yan, W.-D. Oh, and T.-T. Lim, "Low-temperature synthesis of graphene/Bi2Fe4O9 composite for synergistic adsorption-photocatalytic degradation of hydrophobic pollutant under solar irradiation,"*Chemical Engineering Journal*, vol. 262, pp. 1022-1032, 2015/02/15/ 2015, doi: https://doi.org/10.1016/j.cej.2014.10.037.

[22] P. Chaware, A. Nande, S. J. Dhoble, and K. G. Rewatkar, "Structural, photoluminescence and Judd-Ofelt analysis of red-emitting Eu3+ doped strontium hexa-aluminate nanophosphors for lighting application,"*Optical Materials*, vol. 121, p. 111542, 2021/11/01/ 2021, doi: https://doi.org/10.1016/j.optmat.2021.111542.

[23] V. B. Pawade and S. J. Dhoble, "Novel blue-emitting SrMg2Al16O27:Eu2+ phosphor for solid-state lighting,"*Luminescence*, vol. 26, no. 6, pp. 722-727, 2011, doi: https://doi.org/10.1002/bio.1304.

[24] M. M. S. Sanad and M. M. Rashad, "Tuning the structural, optical, photoluminescence and dielectric properties of Eu2+-activated mixed strontium aluminate phosphors with different rare earth co-activators,"*Journal of Materials Science: Materials in Electronics*, vol. 27, no. 9, pp. 9034-9043, 2016/09/01 2016, doi: 10.1007/s10854-016-4936-0.

[25] P. Hervé and L. K. J. Vandamme, "General relation between refractive index and energy gap in semiconductors,"*Infrared Physics & Technology*, vol. 35, no. 4, pp. 609-615, 1994/06/01/ 1994, doi: https://doi.org/10.1016/1350-4495(94)90026-4.